Biochimica et Biophysica Acta, 1100 (1992) 49–57

BBABIO 43584

The reaction-centre associated cytochrome subunit of the purple bacterium *Rhodocyclus gelatinosus*

Wolfgang Nitschke [a], Ileana Agalidis [b] and A. William Rutherford [a]

[a] *Section de Bioénergétique, Département de Biologie Cellulaire et Moléculaire, CE Saclay, Gif sur Yvette (France) and* [b] *CNRS, UPR A0407, Gif sur Yvette (France)*

(Received 21 October 1991)

Key words: Photosynthesis; Reaction center complex; Purple bacterium; Cytochrome; (*Rh. gelatinosus*)

Isolated chromatophore membranes and purified reaction centre light-harvesting B875 complex from the purple bacterium *Rhodocyclus gelatinosus* have been studied by EPR spectroscopy. Four haems occurring in approximately equal stoichiometries could be distinguished in chromatophores. The position of their g_z peaks, their orientations with respect to the membrane and their electrochemical properties have been characterized ($g_z = 3.40$, $E_m = 320 \pm 30$ mV, 0°; $g_z = 3.40$, $E_m = 70 \pm 20$ mV, 0°; $g_z = 3.30$, $E_m = 130 \pm 20$ mV, 90°; $g_z = 3.15$, $E_m = 300 \pm 20$ mV, 90°). At ambient potentials where only the high potential haems are reduced (> +200 mV), the stable photooxidation of the +300 mV haem occurred in a fraction (40%) of centres. Chemical prereduction of the +130 mV haem allows stable charge separation at 4 K in all of the centres. In the case where all four haems are reduced prior to illumination, a subsequent stable photoxidation (at 4 K) of another haem seems to occur, resulting in trapping of the reduced states of both the primary quinone acceptor Q_A and bacteriopheophytin.

Introduction

The core of the photosynthetic reaction centre in purple bacteria seems to be made up from three highly conserved protein subunits, the so-called L-, M- and H-subunits [1]. In many species this set of subunits is complemented by a cytochrome subunit which is attached to the reaction centre on the periplasmic side of the membrane and acts as the immediate electron donor to the special pair bacteriochorophylls (for an overview see Ref. 2).

In fact, an early study on the competence of whole cells to support light-induced photooxidation of haems down to 77 K, which was taken as a criterion for the presence of a reaction centre associated cytochrome subunit, suggested that *most* purple bacteria actually contain such a subunit [3]. This point of view has recently gained further support from comparative studies by Matsuura et al. [2].

By far the best characterized purple bacterial cytochrome subunit is that of *Rhodopseudomonas viridis*, due to the availability of a crystal structure for the *Rps. viridis* reaction centre [1]. This structure showed that the cytochrome subunit contained *four* haems arranged in a linear row protruding into the periplasmic space.

The structure for this tetrahaem cytochrome as seen in the crystal structure, however, was different from a previously proposed model for the reaction centre associated tetrahaem cytochrome of the purple sulphur bacterium *Chromatium vinosum* [4]. This model, which was mainly based on EPR data collected on chromatophores from this bacterium, suggested the presence of two parallel and identical pathways of electron donation to the photooxidized primary donor, the so-called special pair of bacteriochlorophylls.

After the X-ray structure of the *Rps. viridis* reaction centre was published, several groups set out to assign spectroscopic and electrochemical parameters to the four haems seen in the structure [5–9]. The present consensus is that the haems seem to be arranged in the order:lowest potential → second highest potential → second lowest potential → highest potential → special pair, i.e., in an alternating sequence of low- and high potential haems, which is in puzzling contrast to that which would be expected on the basis of 'downhill' electron transfer to the reaction centre. The interposi-

Abbreviations: E_m, redox midpoint potential at pH 7.0; EPR, electron paramagnetic resonance; Mops, 3-*N*-morpholinopropanesulphonic acid; PMSF, phenylmethylsulphonylfluoride; RC, reaction centre complex.

Correspondence (present address): W. Nitschke, Institut de Biologie Physico-Chimique, 13 rue P. & M. Curie, 75005 Paris, France.

tion of a low-potential haem between two high-potential haems seems to be especially unfavourable for electron transport from the second highest to the highest potential haem, which nevertheless occurs at a relatively high rate ($\simeq 3$ μs; Refs. 10, 11).

In summary, the physiological advantage conferred by the tetrahaem cytochrome and its mechanism are still not understood.

Whereas the intensively studied cytochrome subunits from *Rps. viridis* and *C. vinosum* were almost indistinguishable with respect to their redox properties, the analogous cytochrome in *Rhodocyclus gelatinosus* appeared to be rather different. Among the most obvious differences were the lack of a clearcut distinction into low- and high-potential pairs of haems and the ability to photooxidize a high-potential haem at cryogenic temperatures [13].

Thus, the *Rc. gelatinosus* cytochrome subunit appeared to be an interesting system in several respects. In this work we report the electrochemical and orientation characteristics of this multihaem protein as studied by EPR and compare them to those found in *Rps. viridis*.

Materials and Methods

Cultures of *Rc. gelatinosus* (strain 52) were grown as previously described [14], harvested and stored at −80°C. It turned out to be essential to harvest cells in the early logarithmic growth phase in order to obtain less viscous chromatophore samples.

Thawed or unfrozen (in the case of redox titrations) cell paste was resuspended in 20 mM Mops (pH 7.2), 0.1 M NaCl and subsequently disrupted by passing through a French press cell or by a Ribi valve fractionator in the presence of DNase and 1 mM PMSF.

Chromatophores were sedimented by ultracentrifugation and used immediately avoiding any further storage.

Fully oxidized samples were obtained by adding potassium ferricyanide at 1 mM to the chromatophore suspension followed by ultracentrifugation, resuspending in buffer and renewed sedimentation in the ultracentrifuge.

The reaction centre light-harvesting B875 complexes were prepared according to Agalidis et al. [14]. The amount of haem bound to the complex was determined by the pyridine haemochromogen method [15] and the amount of active RC in the complex was estimated from the reversible absorbance decrease at 600 nm, induced by illumination with continuous saturating actinic light ($\Delta\varepsilon = 20$ mM^{-1}cm^{-1}; Ref. 13). A *c*-type haem/RC ratio of 4.19 ± 0.4 (average of 6 experiments) was found. No *b*-type haem was detectable in the respective fractions.

Redox poising and redox titrations of the chromatophore samples (in 50 mM Mops (pH 7.0)) were performed in near darkness under an appropriate safelight essentially as described by Dutton [13]. The following redox mediators were used: 1,4-benzoquinone, *N,N,N',N'*-tetramethyl-*p*-phenylenediamine, diaminodiurol, variamine blue, toluylene blue, 1,4-naphthoquinone, 5-hydroxy-1,4-naphthoquinone, duroquinone, indigo tetrasulphonate, 1,4-dihydroxynaphthoquinone, 2,5-dihydroxy-*p*-benzoquinone, indigo carmine, 2-hydroxy-1,4-naphthoquinone and safranine T at 100 μM, ferricyanide at 10 μM, phenazine methosulphate and phenazine ethosulphate at 50 μM. Reductive titrations were carried out using sodium dithionite and oxidative titrations were done using porphyrexide.

Oriented membrane multilayers were obtained by using the technique of Blasie et al. [16]: chromatophores suspended in H_2O were painted on mylar sheets and were dried in 90% humidity atmosphere for approx. 24 h in darkness at 4 °C. The redox state in these membranes was adjusted by applying solutions of sodium ascorbate and sodium dithionite (in 50 mM Mops (pH 7.0)) to the dried membranes followed by drying under a stream of argon gas in darkness. All angles are defined with respect to the membrane plane. EPR spectra were recorded at liquid helium temperatures with a Bruker ER 300 X-band spectrometer, fitted with an Oxford Instruments cryostat and temperature control system.

Illumination in the EPR cavity was carried out by using an 800 W tungsten projector providing 16000 μE m^{-2} s^{-1} of white light at the EPR cavity window after being filtered through 2 cm of water and two Calflex filters to remove infrared radiation.

Results

Spectral properties of the reaction-centre-associated haems

Fig. 1a shows EPR spectra in the region of the low-spin g_z peaks recorded on chromatophores from *Rc. gelatinosus*. Two separate signals could be distinguished peaking between $g = 3.40$ and $g = 3.30$ and at $g \simeq 3.16$ (the actual position of this peak is at $g = 3.15$, as shown below; in the fully oxidized membrane it appears slightly shifted towards higher *g*-value due to overlap with the other signals). The peak around $g = 3.4$ showed about the same intensity as the line at $g = 3.15$. Since the line intensity is inversely proportional to *g*-value for g_z lines of low spin haems [17], this indicated that more than one haem might contribute to this signal.

Derivative-shaped g_y lines could be observed at $g = 2.11$ and $g = 2.10$ (Fig. 1a).

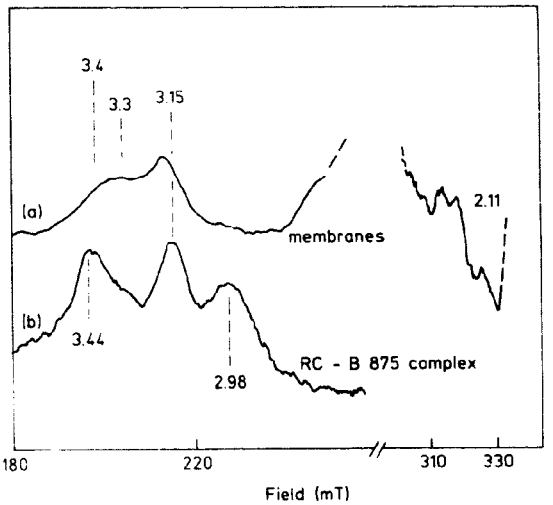

Fig. 1. EPR spectra taken on completely oxidized samples of (a) isolated chromatophores and (b) purified RC light-harvesting B875 complex from *Rc. gelatinosus*.Instrument settings: temperature, 15 K; microwave power, 6.7 mW; microwave frequency, 9.45 GHz; modulation amplitude, 2.5 mT.

Electrochemical properties

Few or no signals could be detected below 0 mV. When the potential was raised from −4 mV to +212 mV, the broad signal around $g = 3.35$ appeared. At lower potentials this signal had its maximum at $g = 3.40$, while at higher potentials its maximum was clearly at a lower g-value (Fig. 2).

The titration curve for the $g = 3.30$–3.40 peak (Fig. 4, squares) was not steep enough to represent a single $n = 1$ transition (Fig. 4, broken curve). This inability to fit a single one-electron titration curve to the data points together with the change in peak position is strong evidence for the presence of at least two different g_z signals giving rise to the observed peak. A good fit to the data points could be achieved using two $n = 1$ Nernst transitions at E_m values of +70 mV and +130 mV (Fig. 4, continuous line). The relative contributions of the two components were chosen as 1 ($g_z = 3.40$; $E_m = +70$ mV): 1.25 ($g_z = 3.30$; $E_m = +130$ mV) in line with the theoretically expected values at these two g-values [17]. However, since the respective g-values could not be determined with high accuracy (due to the broad, weak signals), the midpoint potentials obtained have an uncertainty of ± 20 mV.

When the potential was raised from +200 mV to +400 mV, further signals appeared (Fig. 3). The dominant signal peaks at $g = 3.15$ in the redox difference spectrum (Fig. 3). Its titration curve is shown in Fig. 4 (triangles). It could be fitted by a single $n = 1$ Nernst transition with an E_m of +300 mV.

It is of note that in this range of ambient potentials no g_z signals at $g = 2.8$ to 3.0 could be detected, although the presence of a strong signal of ferricyanide (which had to be used in low concentrations as a redox mediator to achieve equilibration around +400 mV) could have obscured weak signals in this region.

An additional broad signal around $g = 3.40$, however, was seen to titrate at potentials between +250 mV and +350 mV (see Fig. 3). From the data points, an E_m value of approx. +320 ± 30 mV was estimated (Fig. 4, circles). Due to the small signal amplitude, it was not possible to obtain a more precise value for its E_m. It is of note, however, that due to the very high g-value of this signal, its spin concentration is not negligible. The stoichiometry of all four species (taking the g-value dependence of the signal amplitudes into account) was calculated to be 1 : 1.1 : 1.1 : 0.8 for the signals at $g_z = 3.15$ ($E_m = +300$ mV), 3.30 ($E_m = +130$ mV), 3.40 ($E_m = +70$ mV) and 3.40 (E_m +320 mV), respectively.

Thus, we consider that the signal at $g = 3.40$, which is induced at high potentials, represents the second of the two high-potential haems. Its high g-value and the resulting low signal amplitude precluded an estimation of its midpoint potential accurate enough to be certain whether it it is higher or lower than that of the $g = 3.15$

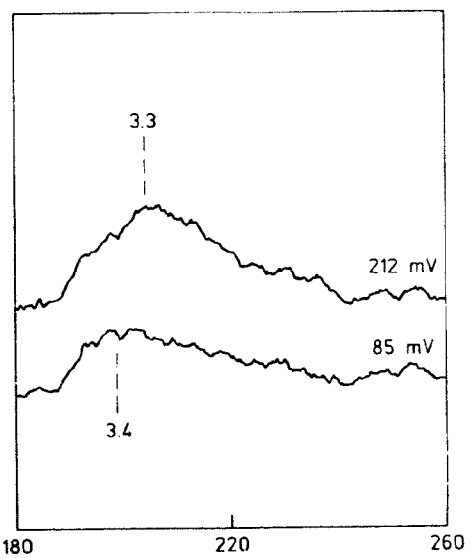

Fig. 2. EPR spectra of chromatophores from *Rc. gelatinosus* taken at two ambient potentials in the range where only the low-potential haems change their redox state. At +85 mV predominantly the lowest potential haem is oxidized, whereas at +212 mV both low-potential haems are fully oxidized. At +212 mV the two high-potential haems are still fully reduced and therefore do not contribute to the spectrum. EPR conditions are as in Fig. 1.

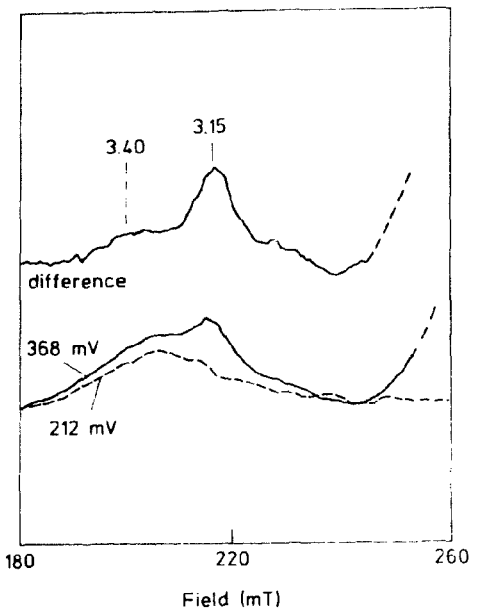

Fig. 3. EPR spectra taken on chromatophores from *Rc. gelatinosus* in the range of ambient potentials where the high potential haems change their redox state. The two lower traces are absolute spectra measured at +212 mV (dashed curve) and at +368 mV (continuous curve). The upper spectrum represents a difference spectrum (+368 mV minus +212 mV, expanded 2-fold). Since at +212 mV both low-potential haems are already fully oxidized, whereas at +368 mV all four haems are oxidized, the difference spectrum shows only contributions arising from the two high-potential haems. EPR conditions are as in Fig. 1.

haem. However, the midpoint potentials of these two higher potential haems are rather close, certainly much closer than those for the two high-potential haems in *Rps. viridis*.

Spectral properties of the RC light-harvesting B875 complex

A typical spectrum of the B875 complex is shown in Fig. 1b. The peaks at $g = 3.15$ and $g = 3.40$, seen in membrane samples (Fig. 1a) were also present in the solubilized complex, but the intensity of the peak at 3.30 seemed to be diminished. Instead, an additional broad signal at $g = 2.95$ to 3.0, the intensity of which varied between samples, could be seen. Since the intensity of this line is smaller than that of any other peak in the spectrum, and since it peaks at the lowest g-value, it represents only a small number of spins compared to the other lines of the spectrum. No signal could be detected in membrane samples at this field position (see Fig. 1a). Thus, we conclude that the peak at $g = 2.95$ to $g = 3.0$ arises from damaged material. A signal at this field position could also be detected in oriented chromatophore samples (see Orientation), which again might be due to the harsh treatment the sample undergoes during drying. Equivalent damage-induced peak shifts to lower g-values have been observed in *Rps. viridis* [7].

Orientation of the haems

Four main peaks could be observed in the magnetic field region expected for the g_z peaks of low spin haems in oriented samples of FeCy-washed membranes from *Rc. gelatinosus* (Fig. 5a). The broad line around $g = 3.4$ showed a complex orientation behaviour with more than one angular maximum. On turning the sample its position varied between 3.40 and 3.35, once again arguing for more than one haem giving rise to this peak (see below). The peak at $g = 3.15$, however, was clearly maximal at 0° (see also the polar plots of Fig. 6c). The same orientation maximum was seen for the broad signal at $g = 2.95$. This peak contained contributions from at least two different haems as indicated by the presence of a shoulder on its low field wing. It is of note that the line at $g = 2.95$ was only visible in oriented membranes and in the isolated B875 complex, but could not be detected during the titration of chromatophores. Whereas it was only a minor peak in non-oriented samples of the B875 complex, it is the

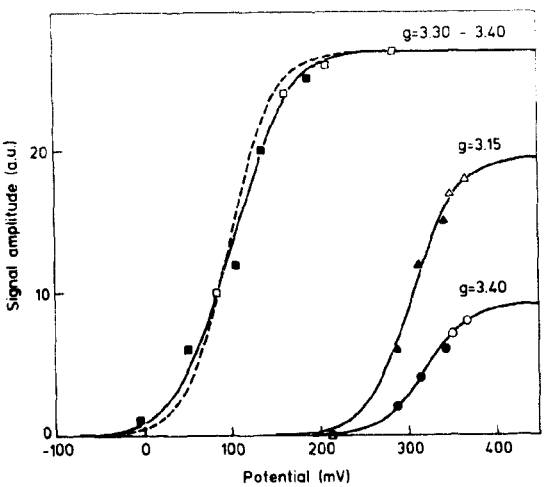

Fig. 4. Redox titration performed on chromatophores from *Rc. gelatinosus* at pH 7.0. The signal amplitude was measured at g = 3.30–3.40 in the lower redox potential range (squares), at $g = 3.15$ (triangles) and at $g = 3.40$ in the high redox potential range (open circles). Data obtained while titrating towards more negative and towards more positive ambient potentials are denoted by filled and open symbols, respectively. For the case of the $g = 3.15$ and the $g = 3.40$ signals the curves drawn represent theoretical $n = 1$ Nernst curves at E_m values of +300 mV and at +320 mV, respectively. For the case of the g = 3.30–3.40 peak at lower ambient potentials, a theoretical one component $n = 1$ Nernst curve is shown as a dashed line, whereas the continuous line represents the superposition of two individual $n = 1$ Nernst curves at midpoint potentials of +70 mV and +130 mV.

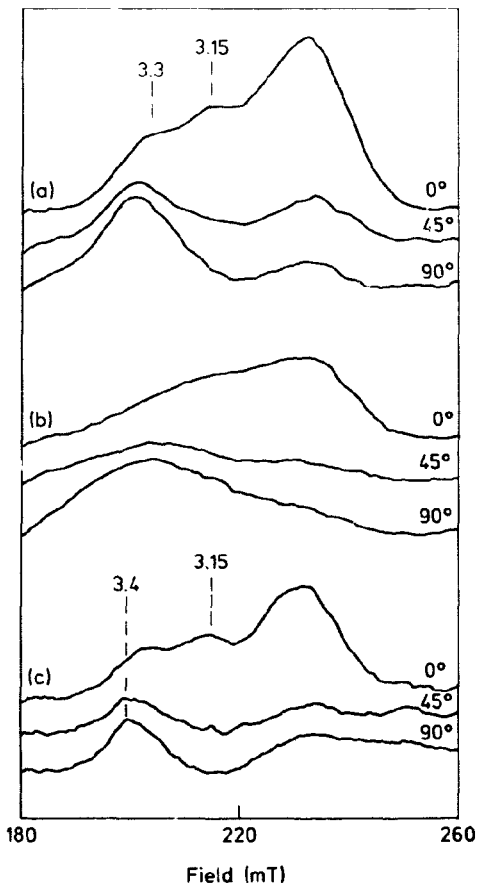

Fig. 5. Orientation dependence of the g_z signals recorded on partially ordered chromatophores from *Rc. gelatinosus*. Spectra were taken on samples in the fully oxidized state (a) and after reduction with sodium ascorbate (b). Spectra shown under (c) represent difference spectra (fully oxidized minus ascorbate reduced). Angles are defined with respect to the membrane plane.

dominant signal in the fully oxidized oriented membrane sample. Signal intensities in oriented samples, however, do not straightforwardly reflect spin concentrations but instead depend strongly on the precise orientations of the respective haems and on their conformational flexibility. Thus, the high signal intensity of the $g = 2.95$ peak in the oriented samples is not necessarily due to further degradation of the sample compared to the B875 complex, but could instead be due to an intensity enhancement caused by the specific orientation dependence of this peak. In any case, the comparison to the non-ordered chromatophore sample strongly suggests that this line is due to damaged haems with an altered EPR spectrum. Therefore, this peak will not be considered in the following discussions.

Chemical reduction of the membrane samples by ascorbate affected all of the peaks (Fig. 5a,b,c), but unequally. Fig. 6a shows the orientation dependence of the low field peak measured at $g = 3.40$. In the oxidized sample the orientation dependence was almost isotropic with an only weakly pronounced maximum at 90° and a less intense additional maximum at 0° (Fig. 6a, filled circles, continuous line). After reduction by ascorbate, the signal intensity was reduced at all orientations, the most prominent decrease occurring at 90° (Fig. 6a, open circles, dot-dashed line). The relative amplitudes of the maxima were inversed in the reduced sample, i.e., the 0° maximum now being more intense than the 90° maximum. The polar plot of the oxidized minus reduced difference spectra demonstrated that predominantly a 90° component was reduced by ascorbate at this g-value (Fig. 6a, triangles, dashed line). This component was attributed to the redox species which titrated around 320 mV at this g-value (see electrochemical properties). The two remaining maxima in the polar plot of the ascorbate reduced sample must therefore arise from the two lower-potential haems seen during the redox titration ($g_z = 3.40$, $E_m = +70$ mV and $g_z = 3.30$, $E_m = +130$ mV). The difference in g-value allowed an attribution of redox- and orientation data by comparing the polar plots of the reduced sample at the two respective g-values. The curve representing the line intensities at the higher g-value emphasized the 90° component whereas the signal intensity measured at the lower g-value had its maximum around 0° (Fig. 6b). Thus, the $E_m = +70$ mV haem (higher g) is parallel to the membrane (g_z at 90°) whereas the +130 mV haem is approximately perpendicular to the membrane (g_z at 0°).

The peak at $g = 3.15$ was nicely oriented parallel to the membrane as seen from the polar plot of the difference spectra (Fig. 6c). The haem giving rise to this spectral component must therefore be perpendicular with respect to the membrane plane.

Photooxidation at cryogenic temperatures

When the sample was poised to ambient potentials where only the high-potential haems were reduced, illumination at low temperature resulted in the stable photooxidation of the haem giving rise to the peak at $g = 3.15$ (Fig. 7, inset, spectrum a). The appearance of the haem g_z signal at $g = 3.15$ was accompanied by the signal of the $Q_A^- Fe^{2+}$ complex (Fig. 7, inset, spectrum a). At potentials below 200 mV, when the lower potential haems become reduced, the photooxidation of the $g = 3.15$ haem is lost (spectrum b). The increase of the semiquinone-iron signal, however, demonstrated that stable charge separation still occured. The appearance of the respective haem signal could not be reliably detected due to the much smaller amplitude of the g_z 3.40 peaks of the lower potential haems.

Therefore, the redox potential dependence of stable charge separation was monitored by plotting amplitudes of the $Q_A^- Fe^{2+}$ signal rather than using the very weak haem peaks (Fig. 7). At potentials below 200 mV (i.e., as the $E_m = +130$mV haem goes reduced), the amount of photoreduced Q_A increased by a factor of 2.5. Assuming that the maximal observed $Q_A^- Fe^{2+}$ signal reflects 100% of the centres, the results indicate that above +200 mV stable charge separation at low temperatures occurs only in 40% of the centres. No further increase of the photoreduced $Q_A^- Fe^{2+}$ signal could be seen below 50 mV. Despite the scatter of the data in Fig. 7, they are roughly in agreement with an $E_m = +130$ mV titration curve (dotted curve), rather than with the $E_m = +70$ mV curve (dot-dashed curve), however, a mean value of +100 mV cannot be ruled out.

A comparable study of light-induced photooxidation using optical methods has been performed by Dutton [13]. According to this study, at $E_h > +200$ mV only a

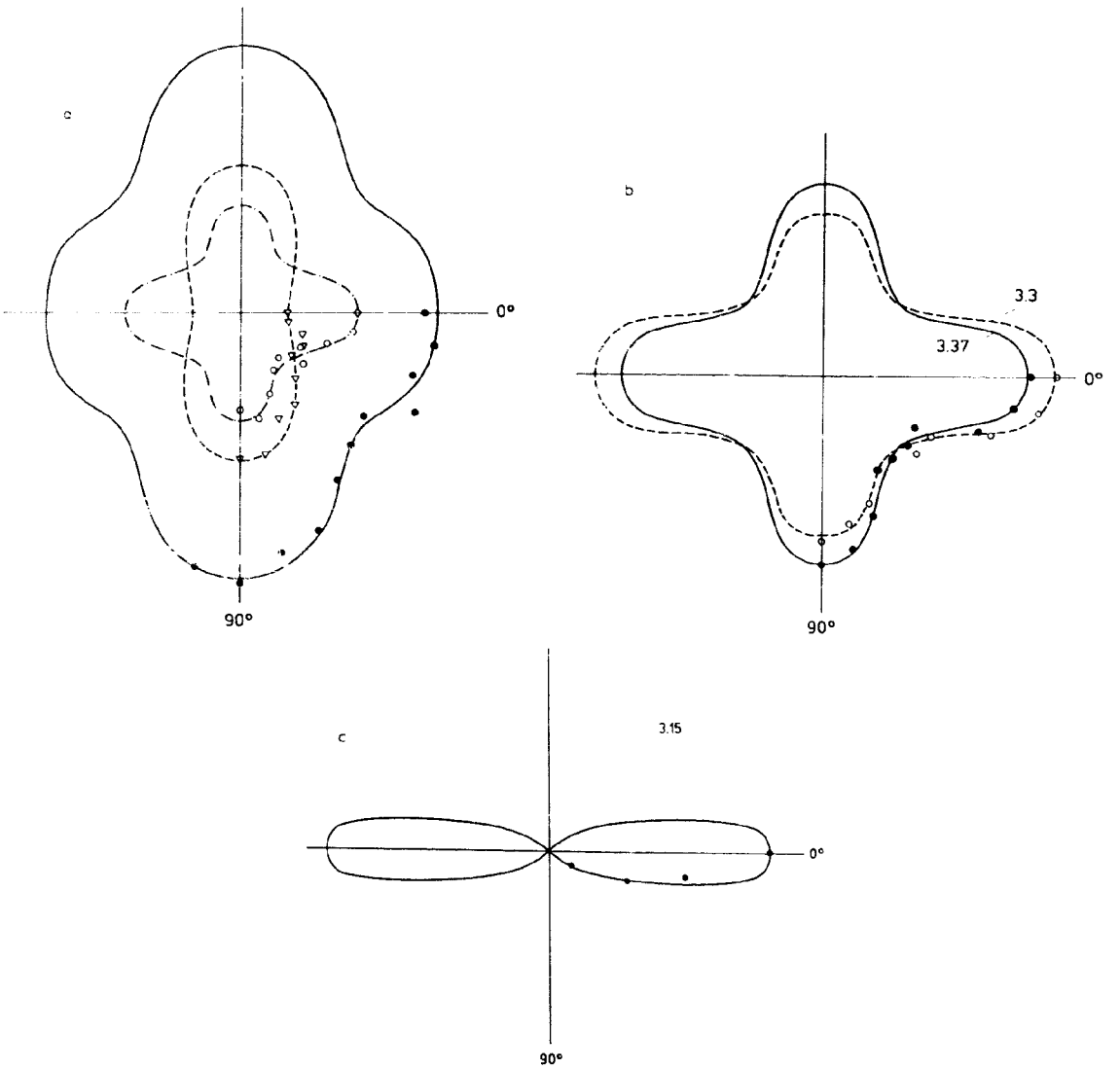

Fig. 6. Polar plots of signal amplitudes measured on the spectra in Fig. 5. The amplitude at $g = 3.40$ from spectra taken on the fully oxidized sample (filled circles, continuous curve), and on the ascorbate-reduced sample (open circles, dot-dashed curve), as well as from the difference spectra (triangles, dashed curve) are shown in (a). (b) compares the orientation dependence of the signal measured at $g = 3.37$ (continuous curve), i.e., emphasizing the +70 mV haem, with that of the same signal measured at 3.30, i.e., emphasizing the +130 mV haem. The orientation dependence of the peak at $g = 3.15$ is shown in (c).

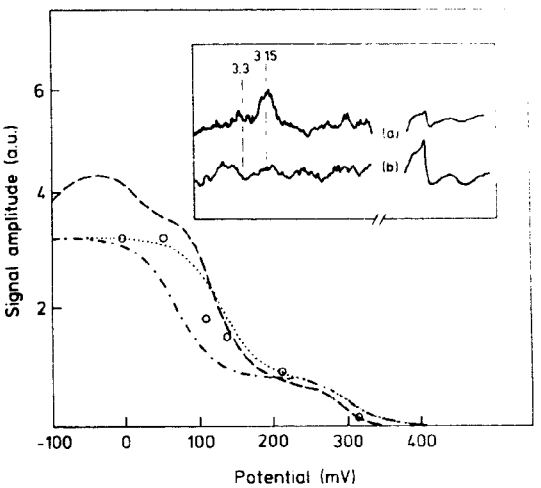

Fig. 7. Redox titration of the Q_A Fe^{2+} signal which is stably photoinduced at 4 K. Theoretical $n = 1$ Nernst curves for $E_m = +130$ mV (dotted line) and $E_m = +70$ mV (dash-dotted line) are superimposed on the data points (open circles). For comparison, the titration curve for the optically monitored stable haem oxidation at 77 K (dashed line), measured by Dutton [13], was normalized to approximately the same amplitude as our curves at +200 mV and included in this figure. The inset shows representative EPR spectra in the region of the haem g_z peaks and the semiquinone-iron signal recorded after 15 minutes illumination at 4 K at +212 mV (a) and at +85 mV (b). EPR conditions for recording spectra of the haems are as in Fig. 1. For the observation of the semiquinone-iron signal, the following conditions were used: temperature, 4.5 K; microwave power, 32 mW; modulation amplitude, 2.2 mT.

fraction of the total photooxidizable haems is *stably* photooxidized at 77 K, whereas the remaining fraction of cytochrome oxidized in the light is rapidly rereduced by a backreaction as soon as the light is switched off. Only when the low-potential haems become chemically reduced prior to the illumination, the full extent of stably photooxidized haems is attained. The respective curve for the optically measured photooxidation of the haems at 77 K as shown in Fig. 6 of [13] was superimposed on our own data in Fig. 7 (broken curve). In addition to the increase around +130 mV, which can be seen in both our and Dutton's data, a further increase of photooxidized haems at potentials below +50 mV was reported by Dutton (yet with a considerably slower halftime of oxidation), which obviously does not correlate to a further increase of the photoreduced $Q_A^-Fe^{2+}$ signal (our data). At potentials below +50 mV, however, light-induced changes in the $g = 2.00$ region could be seen in our spectra which were completely absent above +70 mV (not shown). These spectral changes were due to the formation of the split $BPhe^-$ signal. The intensity of this signal was maximal at about 0 mV.

Therefore, we conclude that at potentials where both low-potential cytochromes were reduced, two haems can be stably photooxidized during the period of illumination resulting in stable trapping of both Q_A^- and $BPhe^-$.

Several attempts to observe the above described photooxidation of haems at low temperature in oriented samples failed. Since even in non-oriented samples, stable charge separation at low temperature was easily lost upon aging of the samples, we consider it quite likely that the native oxidation reactions were too labile to survive the drying process.

The light-induced stable oxidation of a g_z peak at 3.04, however, could be observed in dithionite-reduced, oriented samples. At this g-value no haem signals were present in the non-oriented samples and no photooxidation of haem could be observed throughout the range of ambient redox potentials. Thus, the photooxidized peak at $g = 3.04$ represents a tiny fraction of centres which became only detectable because of their low g-value.

Discussion

Comparisons to other studies

The data indicate the presence of four haems associated with the reaction centre in *Rc. gelatinosus*. These four haems were distinguishable with respect to their orientations and midpoint potentials. Table I summarizes the electrochemical and orientational parameters as well as the low-temperature photochemistry of the four haems.

Two previous studies reported redox midpoint potentials for the reaction centre associated cytochrome of *Rc. gelatinosus* [13, 18]. Fukushima et al. [18] performed optical equilibrium redox titrations on the purified B875 RC-cytochrome complex. Whereas it was found that the complex contained four haems, only two titration waves with apparent potentials of +90 mV and +333 mV were observed. The amplitudes of the two waves were roughly equal, strongly suggesting that each wave contained contributions from two of the four haems in the cytochrome subunit. The haems which titrated at 90 mV were spectrally different (α-peak at 551 nm) from those titrating at 333 mV (α-peak at 555 nm), however within each wave no distinction between the constituents could be made.

The two highest-potential haems seen by EPR ($g_z = 3.40$; $E_m = +320$ mV and $g_z = 3.15$; $E_m = +300$ mV) most probably correspond to the high-potential wave seen in the optical experiment [18]. Their respective midpoint potentials are too close to be distinguishable in an optical experiment if the peak wavelengths are similar. The respective 'non-resolved' potential resulting from our experiments would be +310 mV. Thus, the midpoint potential for the high-potential haems

determined by Fukushima et al. [18] is similar to ours within the limits of our experimental error.

The two haems titrating below 200 mV differ sufficiently with respect to g-value to be discernible. However, even without this spectral difference, the shape of the titration curve excludes the possibility that the two haems have equal midpoint potentials. Again, the mean value of +100 mV which results if the titration curve is fitted by only one Nernst component, is very close to the E_m value of +90 mV determined by Fukushima et al. [18] for the titration wave of cytochrome c_{551}. It is possible that a close inspection of the optical data would equally reveal two distinct components.

Dutton [13] measured the dependence of photooxidizability of haems at 77 K versus ambient redox potential. In contrast to all other examined species [19] *Rc. gelatinosus* was found to be able to perform this reaction already at moderately high ambient potentials (350–250 mV). An E_m of +280 mV for both the reversible and the irreversible cytochrome oxidation seen in the optical experiments was determined. Under the same conditions we see the $g_z = 3.15$ haem going photooxidized. However, due to the intrinsically small signal amplitude of the $g_z = 3.4$ haem, a contribution of this haem can not be ruled out.

At potentials below 150 mV the extent of optically determined haem photooxidized at 77 K further increased [13] and the same effect was monitored here at 5 K for the photoreduction of Q_A in EPR (Fig. 7). Dutton determined an E_m value of +130 mV for this reaction. From our data on Q_A photoreduction we would not be able to distinguish unambiguously between a titration curve with an E_m of +130 mV (i.e., only the +130 mV haem contributes to this reaction) or with an E_m of +100 mV (i.e., both haems equally contribute). However, since the optical data clearly indicate an E_m of +130 mV, we conclude that it is sufficient to reduce this haem in order to obtain 100% stable charge separation at low temperature.

This conclusion allows us to reconcile the apparent discrepency between the E_m of +130 mV reported by Dutton [13] and that of +90 mV reported by Fukushima et al. [18], since Dutton's experiments reflect low-temperature photooxidation whereas Fukushima's data are based on equilibrium redox titrations.

Interestingly, an additional increase of the extent of photooxidizable haem occurred below 100 mV in Dutton's optical experiment. Three different arguments suggest that this additional increase is due to two sequential oxidations of cytochrome leading to phototrapping of both Q_A^- and $BPhe^-$. (1) The titration curve seen in Dutton's work for this 'slowly' oxidized cytochrome coincides well with the titration curve of the ($g_z = 3.40$) $E_m = +70$ mV haem. (2) No further increase in photoreduced Q_A was seen by EPR at these potentials. (3) The split signal of the interacting $BPhe^-$ radical [20] could be detected after prolonged illumination at these ambient redox potentials.

From Dutton's data, it seems likely that this behaviour occurs only in the fraction of centres which are competent in irreversible cytochrome oxidation at high redox potentials. In addition, it is probably relevant that the electron donation kinetics of the low potential cytochromes in *Rc. gelatinosus* are faster ($t_{1/2}$ of 5 μs at 77 K, Ref. 21) than in *Rps. viridis* (20 μs at 77 K, Ref. 22).

Comparison to Rps. viridis

Similar to *Rps. viridis*, the four haems found in the *Rc. gelatinosus* subunit are all distinguishable with respect to orientation and redox midpoint potentials.

Unlike the situation found in *Rps. viridis*, *Rc. gelatinosus* is able to perform stable photooxidation at cryogenic temperatures of the RC-associated haems even at potentials where only the high-potential haems are reduced. This stable photooxidation, however, occurs only in a fraction of the centres, implying heterogeneity inherent in the sample. A corresponding heterogeneity

TABLE I

Spectral, electrochemical and orientational parameters of the four haems associated with the Rc. gelatinosus reaction centre

g_z	E_m (mV)	Angle of heme to membrane	Stable low T photooxidation	Optical α-peak [a,b] (nm)
3.40	320 ± 30	0°	?	555 (553)
3.40	70 ± 20	0°	(+ +)	551 (549)
3.30	130 ± 20	90°	+ +	551 (549)
3.15	300 ± 20	90°	+	555 (553)

[a,b] The wavelengths of the optical α-peaks are taken from Fukushima et al. [18] and Dutton [13]. The values in brackets represent the respective wavelengths measured at 77 K.

may explain some of the low temperature electron donation phenomena observed in *Rps. viridis*. A similar suggestion has been made already [23], but an alternative explanation involving a temperature dependent redox equilibrium has also been put forward [22]. It is clear, though, that in *R. gelatinosus*, such a redox equilibrium mechanism cannot account for the experimental results.

On the basis of the present experimental data, a structural model stipulating a haem sequence cannot be given. However, if a high-low-high-low-potential sequence is assumed in *Rc. gelatinosus*, the less marked potential steps may be responsible for some of the differences seen in the low temperature photochemistry compared to *Rps. viridis*.

Acknowledgements

The authors would like to thank Drs. G. Alegria (Philadelphia), S.M. Dracheva (Tempe), P.L. Dutton (Philadelphia), P. Mathis (Saclay), A. Verméglio (Cadarache), for communicating results prior to publication and F. Reiss-Husson for stimulating discussions. Porphyrexide was kindly provided by M. Denis (Marseilles) and H. Beinert (Milwaukee). A.W.R. and I.A. are supported by the CNRS (URA 1290 and UPR A0 407).

References

1 Deisenhofer, J. and Michel, H. (1989) EMBO J. 8, 2149–2169.
2 Matsuura, K. and Shimada, K. (1990) in Current Research in Photosynthesis, Vol. 1 (Baltscheffsky, M., ed.), pp. 193–196, Kluwer, Dordrecht.
3 Kihara, T. and Chance, B. (1969) Biochim. Biophys. Acta 189, 116–124.
4 Tiede, D.M., Leigh, J.S. and Dutton, P.L. (1978) Biochim. Biophys. Acta 503, 524–544.
5 Dracheva, S.M., Drachev, L.A., Zaberezhnaya, S.M., Konstantinov, A.A., Semenov, A.Yu. and Skulachev, V.P. (1986) FEBS Lett. 205, 41–46.
6 Verméglio, A., Richaud, P. and Breton, J. (1989) FEBS Lett. 243, 259–263.
7 Nitschke, W. and Rutherford, A.W. (1989) Biochemistry 28, 3161–3167.
8 Fritzsch, G., Buchanan, S. and Michel, H. (1989) Biochim. Biophys. Acta 977, 157–162.
9 Alegria, G. and Dutton, P.L. (1991) Biochim. Biophys. Acta 1057, 258–272.
10 Shopes, R.J., Levine, L.M.A., Holten, D. and Wraight, C.A. (1987) Photosynth. Res. 12, 165–180.
11 Dracheva, S.M., Drachev, L.A., Konstantinov, A.A., Semenov, A.Yu., Skulachev, V.P., Aruntjunjan, A.M., Shuvalov, V.A. and Zaberezhnaya, S.M. (1988) Eur. J. Biochem. 171, 253–264.
12 Knaff, D.B., Willie, A., Long, J.E., Kriauciunas, A., Durham, B. and Millet, F. (1991) Biochemistry 30, 1303–1310.
13 Dutton, P.L. (1971) Biochim. Biophys. Acta 226, 63–80.
14 Agalidis, I., Rivas, E. and Reiss-Husson, F. (1990) Photosynth. Res. 23, 249–255.
15 Basford, R.E., Tisdale, M.D., Gleen, J.L. and Green, D.E. (1957) Biochim. Biophys. Acta 24, 107–115.
16 Blasie, J.K., Erecinska, M., Samuels, S. and Leigh, J.S. (1978) Biochim. Biophys. Acta 501, 33–52.
17 De Vries, S. and Albracht, S.P.J. (1979) Biochim. Biophys. Acta 546, 334–340.
18 Fukushima, A., Matsuura, K., Shimada, K. and Satoh, T. (1988) Biochim. Biophys. Acta 933, 399–405.
19 Dutton, P.L. and Prince, R.C. (1978) in The Photosynthetic Bacteria (Clayton, R.K. and Sistrom, W.R., eds.), pp. 525–570, Plenum Press, New York.
20 Tiede, D.M., Prince, R.C. and Dutton, P.L. (1976) Biochim. Biophys. Acta 449, 447–467.
21 Kihara, T. and McGray, J.A. (1973) Biochim. Biophys. Acta 292, 297–309.
22 Kaminskaya, O., Konstantinov, A.A. and Shuvalov, V.A. (1990) Biochim. Biophys. Acta 1016, 153–164.
23 Gao, F.-L., Shopes, R.J. and Wraight, C.A. (1990) Biochim. Biophys. Acta 1015, 96–108.